

Supporting Information

Self-assembly of tripeptides into γ -turn nanostructures

Yumi Ozawa,^a Hisako Sato,^b Yohei Kayano,^c Nana Yamaki,^d Yuichiro Izato,^d Atsumi Miyake,^e
Akira Naito,^a Izuru Kawamura^{*a,c}

^{a.} Graduate School of Engineering, Yokohama National University, Hodogaya-ku,
Yokohama 240-8501, Japan,

^{b.} Department of Chemistry, Graduate School of Science and Engineering, Ehime
University, Matsuyama 790-8577, Japan,

^{c.} Graduate School of Engineering Science, Yokohama National University,
Hodogaya-ku, Yokohama 240-8501, Japan,

^{d.} Graduate School of Environment and Information Sciences, Yokohama National
University, Hodogaya-ku, Yokohama 240-8501, Japan,

^{e.} Institute of Advanced Sciences, Yokohama National University, Hodogaya-ku,
Yokohama 240-8501, Japan.

*Corresponding author: izuruk@ynu.ac.jp

Table of contents

1. Materials and Methods	S-2
2. Structural formulas of a zwitterionic state of FFF , fFF , FfF , FFf (Scheme S1) ...	S-5
3. RP-HPLC chart of FFf (Figure S1)	S-6
4. SEM images (Figure S2).....	S-7
5. TG measurements (Figure S3).....	S-8
6. Observed and calculated VCD (Figure S4 and S5).....	S-9, S-10
7. ¹³ C solid-state NMR spectra (Figure S6).....	S-11
8. The γ -turn structure with the backbone dihedral angles (Figure S7)	S-12
9. Possible formations of hydrogen bonds (Figure S8)	S-13
10. Table S1-S4	S-14, S-15, S-16

Material and methods

Synthesis of peptide and the way of self-assembly

L-Phe-L-Phe-L-Phe-OH (**FFF**), D-Phe-L-Phe-L-Phe-OH (**fff**), L-Phe-D-Phe-L-Phe-OH (**FfF**), L-Phe-L-Phe-D-Phe-OH (**Fff**), and their enantiomers, D-Phe-D-Phe-D-Phe-OH (**fff**), L-Phe-D-Phe-D-Phe-OH (**Fff**), D-Phe-L-Phe-D-Phe-OH (**fff**), D-Phe-D-Phe-L-Phe-OH (**fff**) were carefully synthesized while suppressing a racemization using low microwave output (xx W) by microwave-assisted solid-phase peptide method using an Initiator+ Alstra peptide synthesizer (Biotage). We used Fmoc-L-Phe and Fmoc-D-Phe amino acids and the L-Phe- and D-Phe- loaded resins purchased from the WATANABE CHEMICAL INDUSTRIES, LTD. Then, we cleaved the peptide from the resin by treating 95% trifluoro-acetic acid (TFA) solution for 2 hours. The peptide was purified by RP-HPLC (Shimadzu Prominence system) equipped with a Kinetex Axia C18 ODS column. The purity of those peptides was > 97% without production of any diastereomers. The peptides were confirmed with its mass number, $[M+H] = 460.49$ m/z, by MALDI-TOF-MS (Bruker Daltonics).

Each peptide was dissolved at a high concentration of 100 mg/mL in 1,1,1,3,3,3 hexafluoro-2-propanol (HFIP) and then the solution was diluted with ultra-pure water kept at 5 °C to a final peptide concentration of 10 mg/mL and kept the temperature at 5 °C during the self-assembly. After adding water, the peptide rapidly self-assembled into white sediments at pH 4.9-5.2. The sample was sufficiently dried and collected by suction filtration at room temperature.

FE-SEM

The morphology of the self-assembled peptide was identified by FE-SEM (HITACHI High-Tech SU-8010). The precipitate was scraped off with a spatula and mounted on a double-side adhesive carbon tape and dried thoroughly at the room temperature. SEM samples were coated with Pt-Pd to improve its electrical conductivity and to prevent sample-charging problems. We also used retarding method to minimize the electrostatic charge effect. The scanning electron microscope was operated at 1.0 kV and the emission current was at 10 μ A.

TG-MS

Thermal analysis with the mass of evolved gas were performed using thermogravimetry-mass spectrometry (TG-MS). The instrumentation was consisted of a simultaneous thermal analyzer (STA2500-YKD26 Regulus, Netzsch), and a mass spectrometer (QMD 403D, Netzsch). 1 mg of sample was loaded into open alumina pan and heated from 30 to 450 °C at 10 °C min⁻¹ with a constant 100 mL min⁻¹ flow of helium (He) gas as the carrier gas. Gaseous decomposition products were transported to the mass spectrometer through a quartz capillary tube held at 230 °C. The mass spectrometer was operated in the Electro Ionization mode with an ion source temperature

of 300 °C, and the electrons are accelerated to 70 eV.

VCD measurements

VCD spectra were measured with a machine developed in our laboratory with corporation of JASCO Co. Ltd., Japan (PRESTO-S-2016 VCD/LD spectrometer). The VCD samples were prepared as a KBr disk (10 mm ϕ) containing ca. 0.5 wt % of self-assembled **FFF**, **fff**, **Fff**, **FFf** and **fff**, **Fff**, **fFf**, **ffF**, respectively. There were several peaks observed in the VCD spectra with the opposite signs between the optical antipode. In KBr solid sample, the LD were also measured. The VCD signals were accumulated from 5000 to 10000 times. No baseline correction was made for the solid samples. The resolution of wavenumber was 4 cm⁻¹.

Computational details

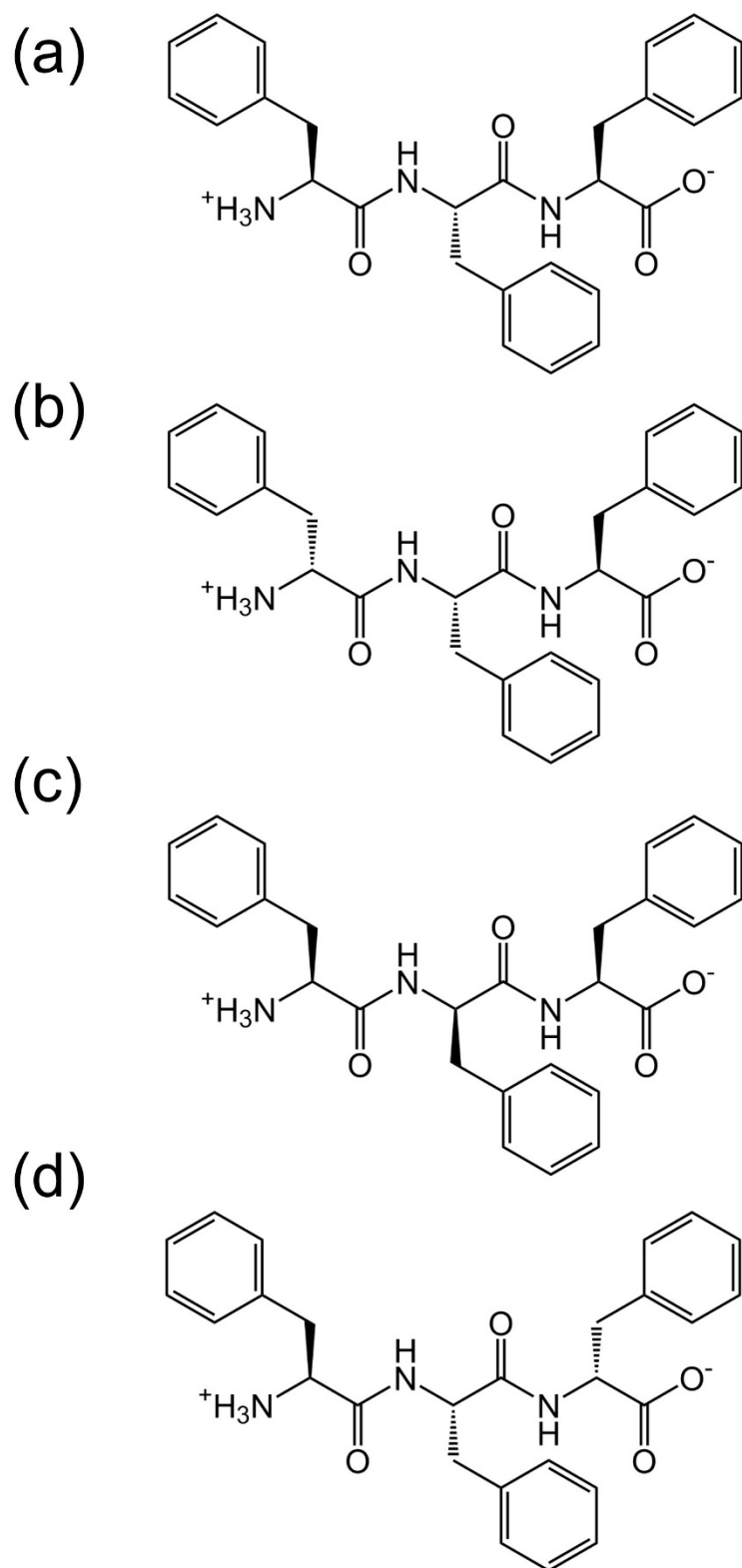
The structures for monomer, dimer and trimer of **FFF** were theoretically calculated by use of Gaussian 16 program (B.01).¹ Geometry optimization was performed at the DFT-d3 level (B3LYP functional and 6-31G(d,p)). After the geometry optimization, IR and VCD were calculated. The VCD intensities were determined by the vibrational rotational strength and the magnetic dipole moments, which were calculated by the magnetic field perturbation (MFP) theory formulated using magnetic field gauge-invariant atomic orbitals. The calculated intensities were converted to Lorentzian bands with 4 cm⁻¹ half-width at half-height.

Solid-state NMR experiments

The self-assembled sample (around 10 mg) was packed into a 4.0 mm o.d. zirconia NMR rotor. ¹³C and ¹⁵N high-resolution solid-state NMR spectra were recorded on a Bruker Avance III (600 MHz) solid-state NMR spectrometer operating at 150.92 and 60.81 MHz for carbon and nitrogen nuclei, respectively, and equipped with a 4.0 mm E-free MAS probe. The typical number of scans was 8000 for ¹³C and 10,000 for ¹⁵N, and the probe temperature was set to 0 °C. Cross Polarization-Magic Angle Spinning (CP-MAS) with a spinal 64 proton decoupling² was performed at a MAS frequency of 10.0 kHz. The ¹³C and ¹⁵N contact times were set to 1.0 and 2.0 ms, respectively. The ¹³C and ¹⁵N chemical shifts were externally referenced to 176.03 and 11.59 ppm for the carbonyl carbon and nitrogen of glycine (tetramethylsilane at 0.0 ppm and ¹⁵NH₄NO₃ at 0.0 ppm). The magnetic field gauge-invariant atomic orbitals (GIAO) ¹H, ¹³C and ¹⁵N NMR chemical shift calculations for optimized structures of **FFF** peptides were calculated as a reference of B3LYP functional and 6-31G(d,p)³.

References

1. M. J. Fisch, et al. Gaussian, Inc., Wallingford CT, 2016.
2. B. M, Fung, et al. J. Magn. Reson. 142, 97-101, 2000.
3. A. Dokalik, et al. Magn. Reson. Chem. 37, 895-902, 1999



Scheme S1. Structural formulas of (a) **FFF**, (b) **fFF**, (c) **FfF** and (d) **FFf** as a zwitterionic state.

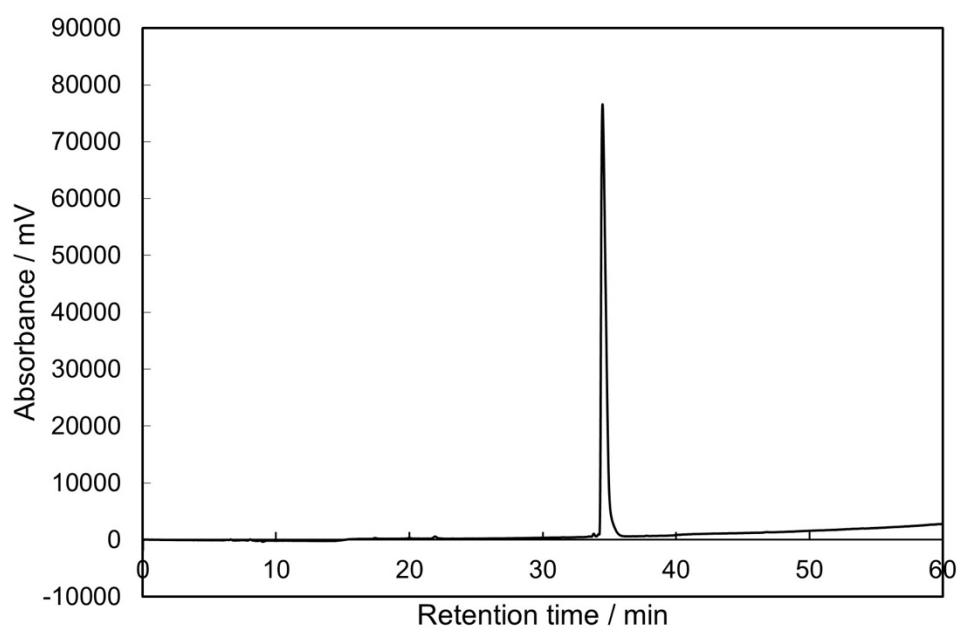


Figure S1. Purification of **FFf** peptide by RP-HPLC. The peptide was eluted with ultrapure water containing 0.02% TFA (solvent A) and 95% acetonitrile containing 0.02% TFA (solvent B), under a linear gradient of solvent B for 60 minutes in the C18 ODS column.

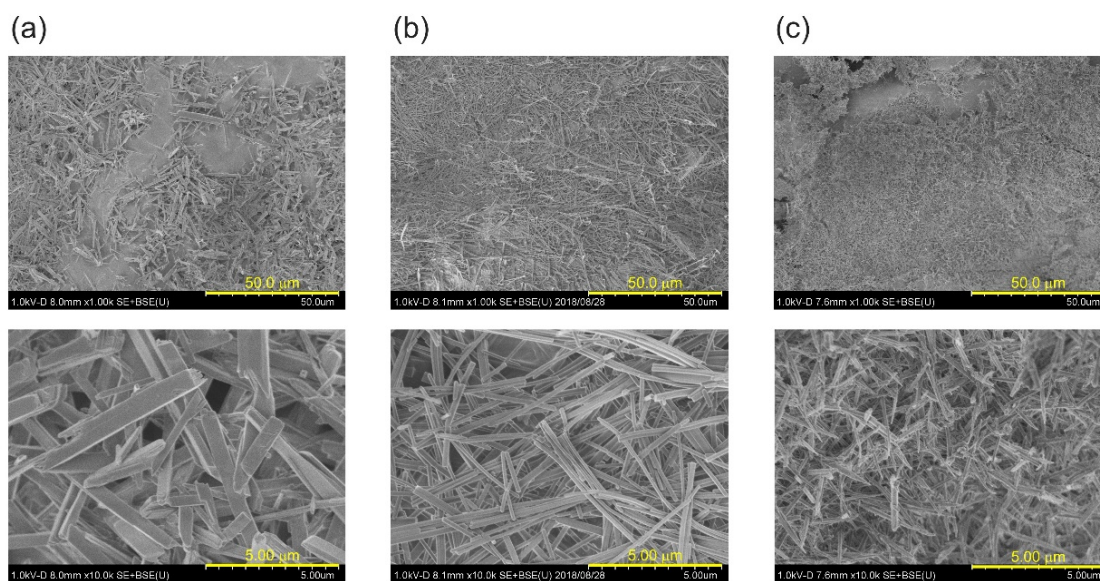


Figure S2. SEM images of (a) **FFF**, (b) **fFF** and (c) **FfF** self-assembled structure on low and high-magnification. The shapes of the self-assembly were observed as nanoplates with width range from 250 to 600 nm and length to 3 μm at least, which are similar with that of **FFf**.

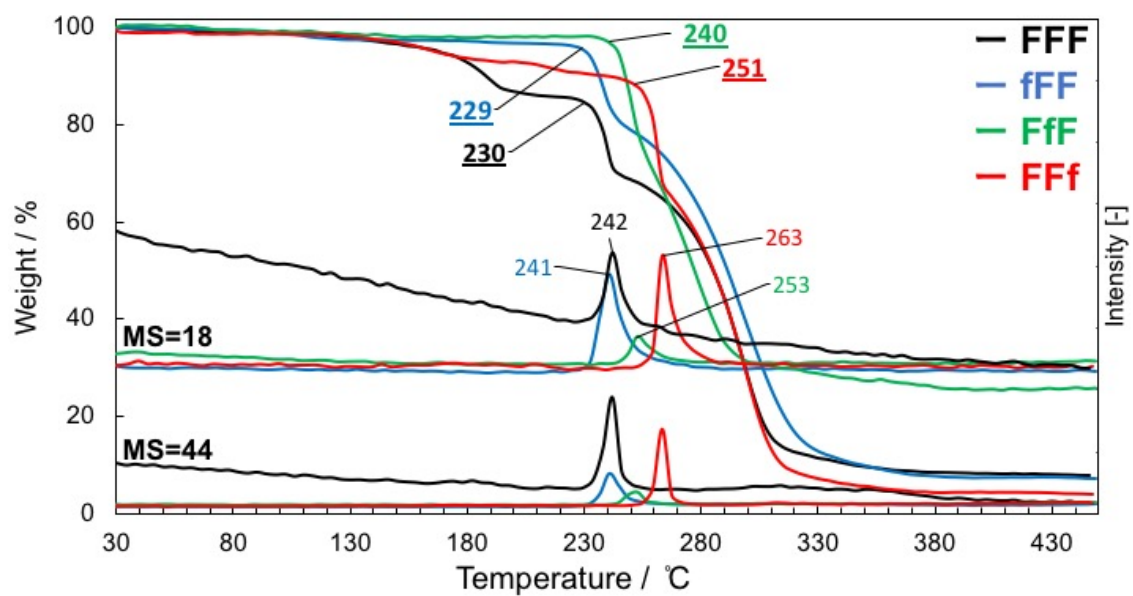


Figure S3. TG curves of **FFF** (black), **fFF** (blue), **FfF** (green) and **FFf** (red) nanoplates recorded at 10 °C min⁻¹ with mass spectrometry (m/z = 18.0 and 44.0).

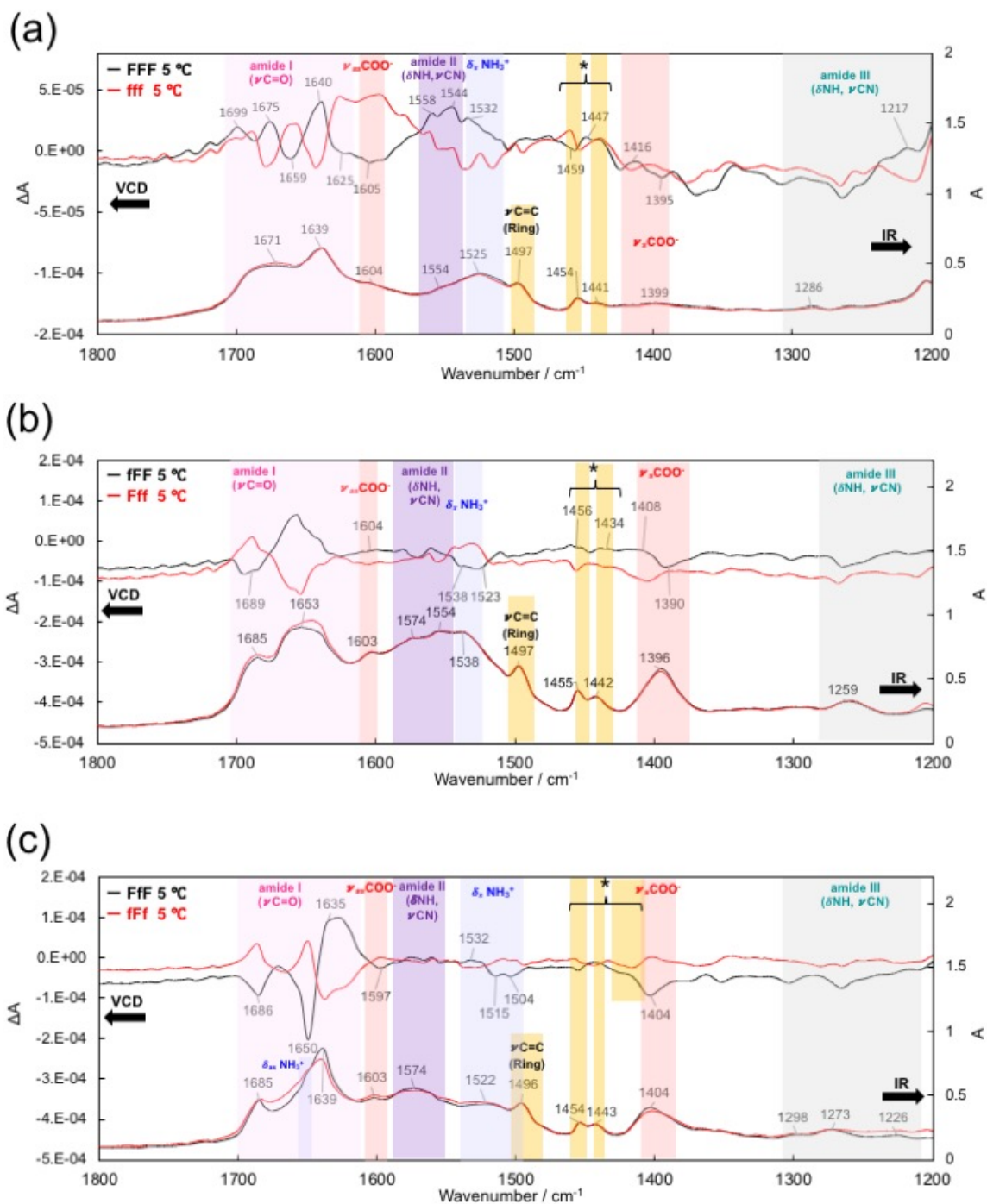


Figure S4. VCD/IR spectra of self-assembled FFF/fff (a), fFF/Fff (b) and Fff/fFf (c). The signals marked with asterisk * indicate the bands of δ C-H($C\alpha$) mixed with N-H bends at around 1455 cm^{-1} , and δ C-H($C\beta$) mixed with aromatic ring C-H at 1442 cm^{-1} .

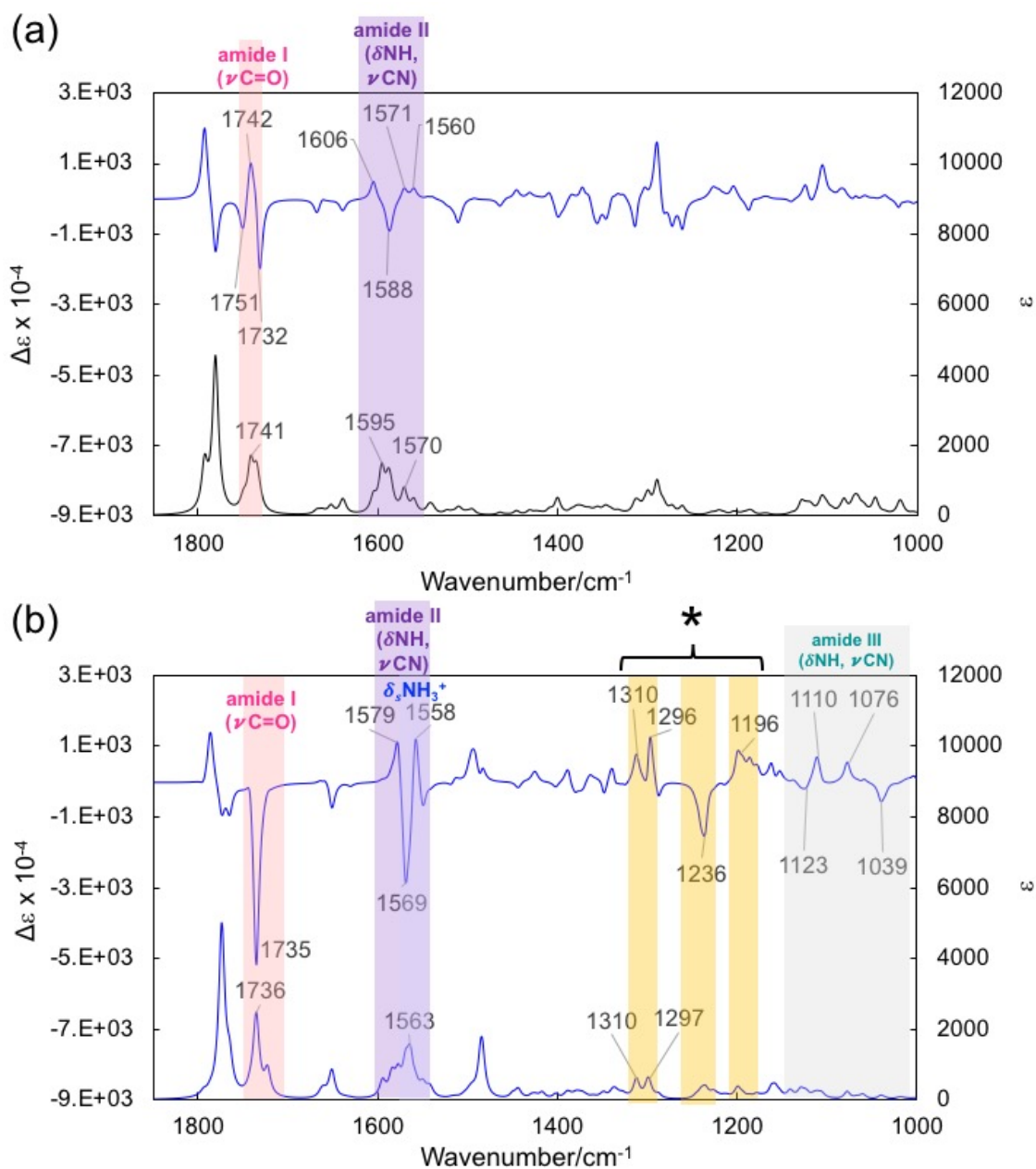


Figure S5. (a) Calculated VCD/IR spectra from optimized structure of three **FFf** peptides. (b) Calculated VCD/IR spectra from manually model of three **FFf** peptides with harmonic vibrations. The signals marked with asterisk * indicate the bands of $\delta\text{C-H}(\text{C}\alpha)$ mixed with N-H bends at 1310 and 1297 cm⁻¹, and $\delta\text{C-H}(\text{C}\beta)$ mixed with aromatic ring C-H at 1236 cm⁻¹, and $\delta\text{C-H}(\text{C}\alpha)$ mixed with $\delta\text{C-H}(\text{C}\beta)$ and aromatic ring C-H at 1196 cm⁻¹.

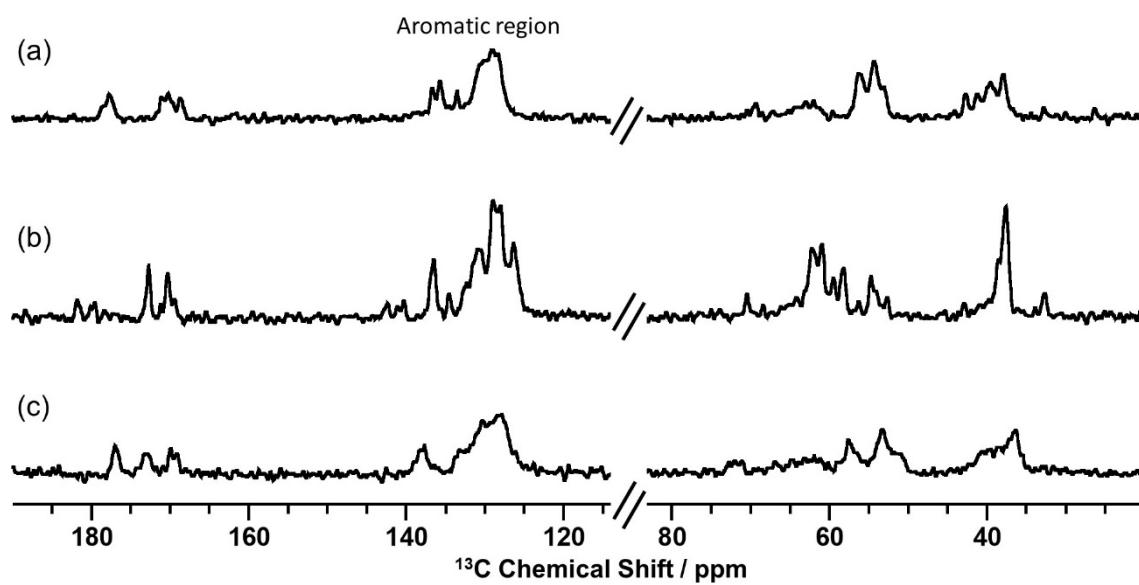


Figure S6. Solid-state ^{13}C CP-MAS NMR spectra of (a) FFF, (b) fFF and (c) FfF nanoplates

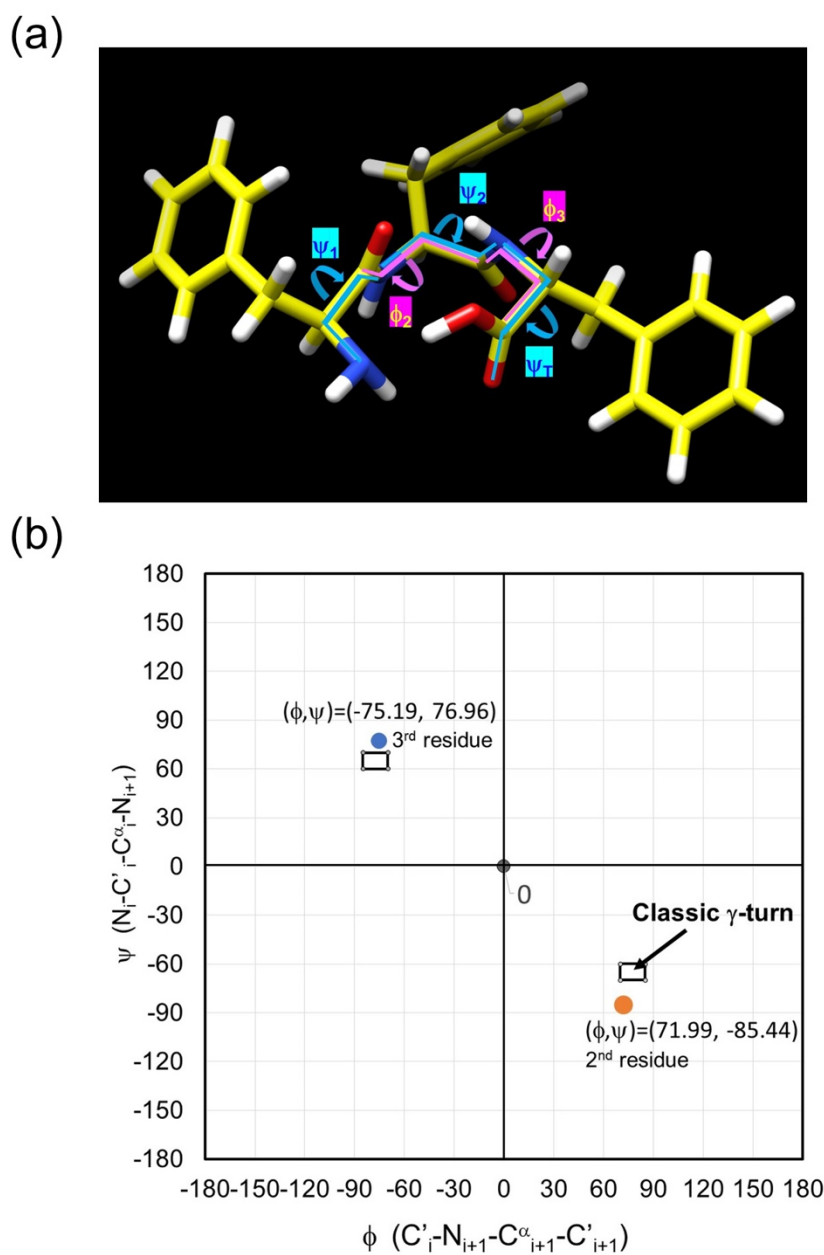


Figure S7. (a) The γ -turn structure of **FFf** with the backbone dihedral angles. ψ_T is $N_3-C^{\alpha}_3-C'_3-O_3$. **(b)** The Ramachandran plot of the **FFf** molecular structure. The small squares in the plot indicate the torsional angles of typical classic γ -turn. Orange circle, the angles of 2nd L-Phe residue. Blue circle, the angles of 3rd D-Phe residue.

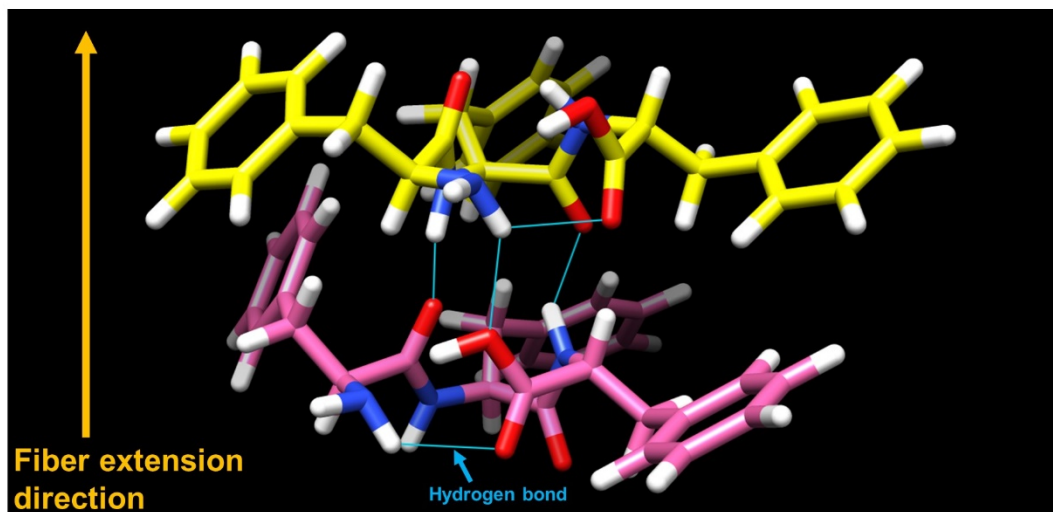


Figure S8. The possible formations of hydrogen bonds of the **FFf** dimer after optimized geometry.

Table S1. IR bands (cm^{-1}) of amide I and amide III of **FFF**, **fFF**, **FfF** and **FFf**.

	FFF	fFF	FfF	FFf
Amide I	1639, 1671	1653, 1685	1639, 1685	1657
Amide III	1286	1253	1226, 1273, 1291	1281, 1304, 1323, 1343
Secondary structure	Anti-parallel β -sheet	Anti-parallel β -sheet	Anti-parallel β -sheet	γ -turn

Table S2. Assignments of IR and VCD signals (cm^{-1}) of **FFf**.

Assignment	Observed value of IR	Observed value of VCD	Observed sign	Calculated value of VCD	Calculated sign
Amide I	1662	1657	-	1735	-
$\nu_{\text{as}}\text{COO}^-$	1596	1592	-	#	#
Amide II	1534	1539, 1509	+, +	1579 1558	+
$\delta_{\text{s}}\text{NH}_3^+$	1522	1523/1509	-/+	1569/1558	-/+
$\nu\text{C}=\text{C}$	1497	#	#	#	#
δ CH($\text{C}\alpha$) mixed with $\delta\text{N-H}$	1454	1455	+	1310 1296	+
δ CH($\text{C}\beta$) mixed with aromatic $\delta\text{C-H}$	1440	1440	-	1236	-
δ CH($\text{C}\alpha$) δ CH($\text{C}\beta$)	#	1422	+	1196	+
$\nu_{\text{s}}\text{COO}^-$	1395	1403/1389	-/+	#	#
Amide III	1343	1343	-	1123	-
	1323	1325	+	1110	+
	1304	1304	+	1076	+
	1281	1282	-	1039	-

Not appeared.

Table S3. Dihedral angles of the model structure as shown in Figure S7.

	ϕ	φ	φ_T
1st residue	-	116.73° (N ₁ -C ^α ₁ -C' ₁ -N ₂)	-
2nd residue	71.99° (C' ₁ -N ₂ -C ^α ₂ -C' ₂)	-85.44° (N ₂ -C ^α ₂ -C' ₂ -N ₃)	-
3rd residue	-75.19° (C' ₂ -N ₃ -C ^α ₃ -C' ₃)	-	76.96° (N ₃ -C ^α ₃ -C' ₃ -O ₃)

Table S4. Observed and calculated ^{13}C and ^{15}N chemical shift values (ppm) of γ -turn-formed **FFf**.

	Signal	Observed chemical shift	Calculated chemical shift
Phe1	$^{13}\text{C}\alpha$	50.55	59.76
	$^{13}\text{C}\beta$	38.07	43.58
	$^{13}\text{C}=\text{O}$	168.89	165.47
	$^{15}\text{NH}_3^+$	22.01	53.70
Phe2	$^{13}\text{C}\alpha$	58.73	63.95
	$^{13}\text{C}\beta$	34.32	34.40
	$^{13}\text{C}=\text{O}$	172.95	164.04
	^{15}NH	101.19	138.29
Phe3	$^{13}\text{C}\alpha$	58.73	62.44
	$^{13}\text{C}\beta$	35.77	37.52
	$^{13}\text{C}=\text{O}$	178.97	169.15
	^{15}NH	106.02	129.71